

NEXT GENERATION SYNCHRONIZATION SYSTEM FOR THE VUV-FEL AT DESY

H. Schlarb*, V. Ayvazyan, F. Ludwig, D. Noelle, B. Schmidt, S. Simrock, A. Winter, DESY, D-22607 Hamburg, Germany and F. Kaertner, MIT, Cambridge, Massachusetts

Abstract

The control and stabilization of the longitudinal beam profile and the bunch arrival time in linac driven VUV or X-ray Free-Electron Lasers requires special effort and new developments in the fields of low-level RF controls, global synchronization systems, and longitudinal beam feedbacks. In this paper we describe the required upgrades for the VUV-FEL at DESY to synchronize the FEL pulse and optical lasers to the hundred femtoseconds (FWHM) level.

INTRODUCTION

Pump-probe configurations are typically used to investigate the evolution of ultrafast systems in atomic physics, chemistry, biology or condensed matter. The time-dependent phenomena is stimulated by a high-power pump pulse, e.g. with an ultrafast optical laser, and then probed after a defined time delay. By repeating the experiment for different delays, the system changes can be recorded and the underlying dynamics understood.

In the standard setup, the pump and the probe beam have a common source, so that precise time delays can be produced with optical path-length differences. The time-resolution can be as short as a fraction of a femtosecond and is limited only by the overlap of the pump and the probe pulses [1, 2].

To carry out pump probe experiments at the VUV-FEL at DESY, a high-power optical laser has been installed. Since the VUV-pulse is generated by passing short electron bunches through a long undulator, the origin of the pump and probe sources is different. Special effort is required to precisely synchronize the electron bunch, thus the FEL-pulse, and the laser pulse to one another. In this paper we discuss the required upgrades of the facility, RF amplitude and phase tolerance and the resolution required of monitor systems serving beam based feedbacks.

VUV-FEL LAYOUT AND TIMING JITTER

The layout of the VUV-FEL is shown in Fig. 1. The electron beam is generated by impinging a laser pulse on an CsTe-photocathode installed in a normal conducting 1.5-cell RF gun. The beam exits the gun with an energy of 4.5 MeV and is accelerated to 130 MeV in the superconducting module ACC1, housing 8 TESLA like cavities. To preserve the electron bunch emittance, the first four cavities are operated at a gradient of 12.5 MV/m. By off-crest acceleration in ACC1, an energy chirp in bunch is introduced, causing a longitudinal compression in the dispersive chicane 'BC2'. Then the energy is raised to 380 MeV by the

cryo-modules ACC2 and ACC3, before the final bunch compression takes place in BC3, an S-shape like chicane. Finally, the electron beam is accelerated to the energy needed to produce a wavelength between 6 nm (1 GeV) and 35 nm (380 MeV). The electron beam passes a collimator system to remove halo before entering the undulator magnets. The FEL beam then passes a 40 m long photon beam line to the experimental hall. The total distance from the RF photoinjector to the FEL experiment is about 260 m.

Presently, the third harmonic cavities (3.9 GHz) to linearize the longitudinal phase space are not yet installed. Thus, the initial, long electron bunch length of about 2 mm entering the ACC1 module receives a significant non-linear energy chirp due to the RF curvature. This causes only a small fraction of the electron beam to be compressed, leading to an ultra-short spike with peak currents of several kA. Strong collective forces such as space charge and coherent synchrotron radiation acting within the spike restrict the linac operation and the FEL pulse duration cannot be tuned.

The observed FEL pulse duration generated by the electron spike can be as short as 25 fs FWHM [3]. For pump probe experiments, ideally the electron beam is synchronized to the range of the photon pulse duration. The rms jitter of the electron bunch arrival time depends primarily on the RF stability and can be expressed as

$$(c_0\sigma_t)^2 = \left(\left[R_{1,56} + \frac{E_1}{E_2} R_{2,56} \right] \frac{\sigma_{V_1}}{V_1} \right)^2 + \left(R_{2,56} \frac{E_2 - E_1}{E_2} \frac{\sigma_{V_2}}{V_2} \right)^2 + \left(\frac{\sigma_{\Phi_1}}{k_{rf}} \right)^2 \quad (1)$$

with V_1 and V_2 being the acceleration voltage of ACC1 and ACC2/ACC3, respectively. The energy and longitudinal dispersion of the first and the second chicane are denoted by $E_1, E_2, R_{1,56}$, and $R_{2,56}$. The RF phase jitter Φ_1 of ACC1 translates directly into the timing jitter of the electron bunch, since in this present compression mode the second acceleration section can not significantly contribute to the energy chirp and is thus operated on-crest ($\Phi_2 = 0$).

With the nominal bending angles of 18° and 3.8° in BC2 and BC3, the ACC1 RF amplitude to beam arrival time conversion is (see Tab.)

$$\sigma_t = 658.1 [ps] \frac{\sigma_{V_1}}{V_1} \quad (2)$$

which dominates the rms jitter budget. For synchronization within the FEL pulse (<10 fs rms), an energy stability of $\sigma_{V_1}/V_1 \approx 1 \cdot 10^{-5}$ is required. This is extremely difficult to achieve and has not been demonstrated for SRF cavities so far. The tolerance on the amplitude stability can be somewhat relaxed by reducing the $R_{1,56}$ in BC2.

* holger.schlarb@desy.de

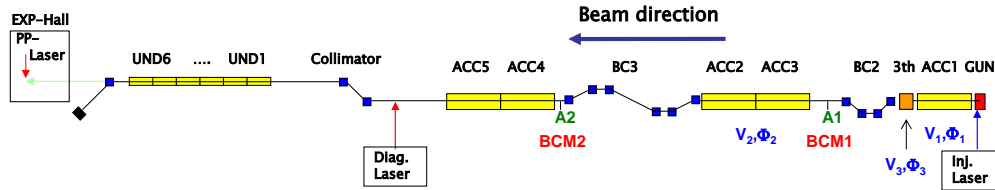


Figure 1: Layout of the VUV-FEL.

Table 1: RF and BC parameters for simulation.

	no 3 th	with 3 th
E_1	130 MeV	130 MeV
E_2	380 MeV	450 MeV
V_1	126.7 MV	148 MV
Φ_1	-8°	-3.9°
V_2	250 MV	368 MV
Φ_2	0°	-29.6°
V_3	-	18.02 MV
Φ_3	-	191.7 MV
$R_{1,56}$	-181 mm	-181 mm
$T_{1,566}$	295 mm	295 mm
$R_{2,56}$	-48.6 mm	-40.0 mm
$T_{2,566}$	73.3 mm	60.2 mm

Achieved energy stability at the VUV-FEL

The energy stability of the first acceleration module has been measured by imaging the beam with an OTR-screen in the straight section of the first bunch compressor. To avoid phase drifts during the measurement and to increase the resolution of the method, the cryo-module has been operated close to on-crest. The screen was calibrated by varying dipole current while monitoring the beam displacement on the screen.

After careful adjustment of the low-level RF parameters, such as loop phase, timing, phase and amplitude offsets, and a re-calibration of the cavity vector sum in the DSP system, shot-to-shot energy stability of $2.8 \cdot 10^{-4}$ could be achieved. Figure 2 shows the energy jitter recorded during 45 min of operation.

The arrival times calculated from this energy jitter amounts to 180 fs rms, in agreement with measurements using spectral-decoding single-shot electro-optical techniques [4].

The measurement represents the energy variation of the first few bunches of each macro-pulse taken at a repetition rate of 2 Hz. The energy stability within a macro-pulse of 800 μ s duration can be much smaller. During superstructure tests (2002, TTF phase 1), the energy stability from macro-pulse to macro-pulse was 0.2%, but a factor of five better result has been achieved within the macro-pulse.

It is planned to replace the RF feedback DSP system by an

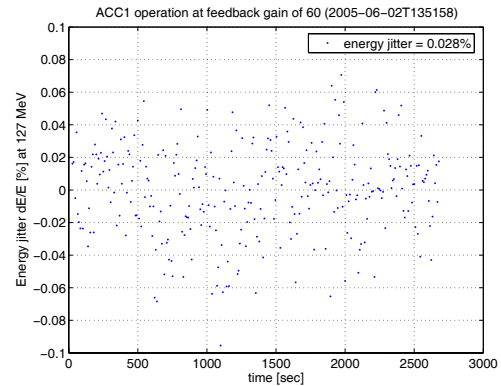


Figure 2: Energy jitter measured in BC2.

FPGA based board and to operated the RF down-converters at an intermediate frequency of 81 MHz instead of 250 kHz. This increases the resolution of the RF measurement and decreases the latency introduced by the data processing. With feedback regulation operated at a higher gain it becomes realistic to stabilize the energy to better than $5 \cdot 10^{-5}$ within the macro-pulse train. In this case, the phase stability of the RF becomes more critical and will dominate the timing jitter unless special care is taken.

Arrival jitter with the 3rd-harmonic cavities

In 2006, four cavities with an operation frequency of 3.9 GHz will be installed between the acceleration module ACC1 and the bunch compressor BC2. At a gradient of 15 MV/m and a length of 0.343 m per cavity, a maximum energy gain of 20.6 MV can be provided. The purpose of the cavities is to remove the non-linear energy-time correlation (chirp) of the bunch caused by the curvature of the 1.3 GHz RF acceleration in ACC1. The non-linear RF effect can be neglected after the beam is compressed in the first chicane.

At BC2 the energy of electrons at position z in the bunch ($z < 0$ bunch head) is

$$E_1 = E_0 + V_1 \cos(k_{rf}z + \Phi_1) + V_3 \cos(3k_{rf}z + \Phi_3), \quad (3)$$

where $(V_1, \Phi_1, V_3, \Phi_3)$ are RF amplitude and phases shown in Fig. 1. The path length of the electrons through the mag-

netic chicane is written by

$$T(E_1) = L_0 + R_{56} \frac{E_1 - E_{10}}{E_{10}} + T_{566} \left(\frac{E_1 - E_{10}}{E_{10}} \right)^2 \quad (4)$$

with $E_{10} \equiv E_1(z=0)$ the energy of the bunch center. The beam energy E_{10} , the linear energy chirp as function of the compression factor C_1

$$E_1' = -\frac{E_{10}}{R_{56}} \left(1 - \frac{1}{C_1} \right) \quad (5)$$

and the compensation for the second order dispersion by a second order energy chirp

$$E_1'' = -2 \frac{T_{566}}{R_{56}} \frac{(E_1')^2}{E_{10}} \quad (6)$$

defines three equations with four RF parameters (V_1, Φ_1, V_3, Φ_3) in Eq. 3. The third order chirp E_1''' is a free parameter and its influence on the final bunch shape and bunch asymmetry is tolerable [5]. As discussed in [5], the third order energy chirp can be chosen such, that the dependency of the beam compression factor on the RF phase jitter for both 1.3 GHz and 3.9 GHz can be entirely removed. But significant RF power is required and the tolerances on the RF amplitudes are tighter. In addition, the sensitivity to arrival time jitter is enhanced, compromising pump probe experiments.

For the VUV-FEL, the parameter E_1''' can only be varied in a small range, due to limitations of the voltage generated by the 3rd-harmonic cavities. The dependence on phase and voltage is plotted in Fig. 3.

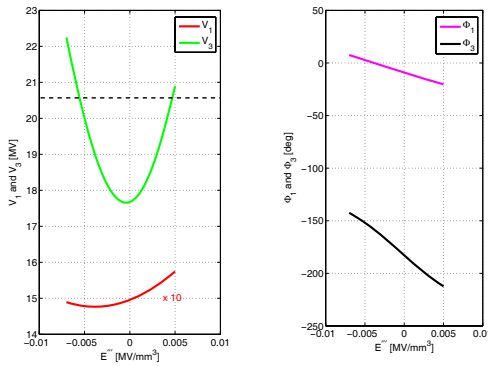


Figure 3: Amplitude and phase in first acceleration section as function of the third order chirp ($C_1 = 5$). Dashed line indicates limit for V_3 .

For pump probe experiments, only the arrival time jitter of the beam behind the last compressor (BC3) is important. This jitter depends on the compression factors C_1 and C_2 , for the first and the second chicane, and the RF stability of modules ACC1 and ACC2-ACC3.

In order to achieve an arrival stability of below 100 fs FWHM, the choice of RF and compression has been selected using the following criteria:

- an rms amplitude tolerance σ_{V_1} of ACC1 $\geq 5 \cdot 10^{-5}$,
- rms phase tolerance σ_{Φ_1} and $\sigma_{\Phi_3} \geq 0.02^\circ$,
- $\sigma_{\Phi_2} \geq 0.06^\circ$, corresponding to timing jitter accuracy requirements for the phase measurement of 1.3 GHz and 3.9 GHz,
- moderate gradients in the acceleration structures (small Lorentz force detuning),
- a weak dependence of arrival time changes on bunch length variations
- independent correction of the arrival time jitter introduced by BC2 and BC3
- decoupling of amplitude and phase from the arrival time jitter.

Finally, the setting should allow a simple variation of the bunch length after BC3 without larger changes in feedback algorithms. A possible set of parameters that fulfill most of the above criteria is listed in Tab. .

Table 2: RF jitter used in simulation. The last two lines lists the conversion factor RF to arrival time after BC2 and BC3. Phase is determined in terms of time jitter (conversion unit [fs/fs])

σ_{V_1}/V_1	σ_{V_3}/V_3	σ_{V_2}/V_2	σ_{Φ_1}	σ_{Φ_3}	σ_{Φ_2}
$5 \cdot 10^{-5}$	$4 \cdot 10^{-4}$	$1 \cdot 10^{-4}$	0.02°	0.06°	0.02°
-684 ps	82 ps	-	-0.40	-0.40	-
-426 ps	51 ps	95 ps	-0.25	-0.25	-0.44

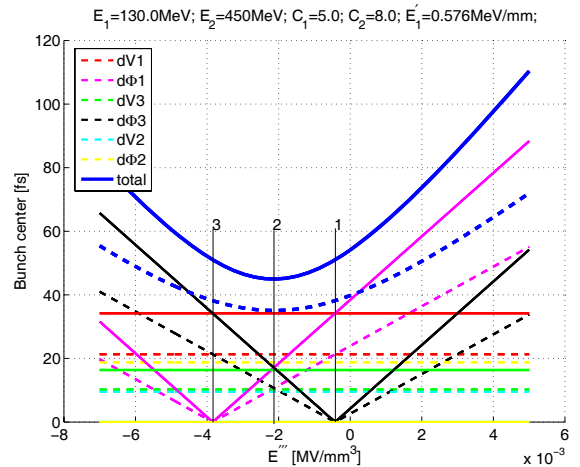


Figure 4: Arrival time jitter of beam behind BC2 (solid) and BC3 (dashed). The rms jitter used in the simulation are listed in Tab. 2

Figure 4 shows the rms arrival time jitter behind BC2 (solid lines) and BC3 (dashed lines) as a function of E_1''' . The effect of different RF parameters are shown, as well

as the overall jitter (blue) assuming that all parameters add independently from one another. The RF jitter for each parameter used in the simulation is listed in Tab. 2 .

The working points 1 or 3, indicated by vertical lines in Fig. 4, show that phase changes of the 3rd-harmonic or the ACC1 module do not contribute. Here, E_1''' is adjusted such that the operation phase is either 180° or 0° for the 3rd-harmonic or ACC1 cavities, respectively..

However, the minimum of the overall jitter is at work point 2, where 50% of the linear energy is generated by ACC1 and 50% by the 3rd-harmonic cavities. The longer bunch at the entrance of ACC2-ACC3 allows for operation of ACC2-ACC3 off-crest in order to compress some of the timing jitter introduced in BC2. The final bunch length is adjustable using Φ_2 , with -29.6° for $\sigma_z = 50 \mu\text{m}$ and -32.5° for $\sigma_z = 20 \mu\text{m}$.

Beam monitoring: The arrival time is dominated by the amplitude stability of ACC1 and the phase stability of ACC2-ACC3. Both have to be measured by arrival time monitors, A1 and A2, shown in Fig. 1. To avoid larger correlated phase changes of Φ_1 and Φ_3 ($\Phi_1 = 3\Phi_3$), or equivalently, an increasing arrival drift of the beam exiting the injector, careful measurement of the energy with BPMs in BC2 is required. An uncorrelated phase jitter ($\Phi_1 = -3\Phi_3$), is the dominant source for bunch length jitter, which is monitored by the bunch compression monitor BCM2. The required accuracy of beam monitors A1 and A2 are 10 fs rms, and for the BPMs in the chicane 10 μm .

NEXT SYNCHRONIZATION SYSTEM FOR VUV-FEL

To achieve the timing jitter for the pump probe experiment, a laser based synchronization system is currently developed at DESY and MIT [6, 7]. Here a brief overview on the various devices, sketched in Fig. 5 will be given. Details and recent results can be found in [8].

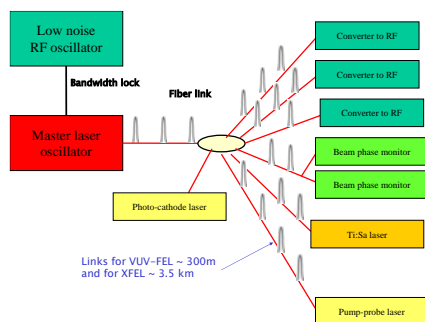


Figure 5: Next generation synchronization system.

Master laser oscillator (MLO): A passive mode-locked, ultra-stable Erbium-doped fiber laser with a repetition rate of 40.625 MHz serves as reference for all timing critical devices. The laser is locked with a piezo-stretcher to an ultra-low noise RF master oscillator. The laser pulses of 0.5 ps

duration (FWHM) and a central wavelength of 1550 nm are distributed in optical path-length stabilized fiber links. The integrated phase noise of the MLO has been measured to be <10 fs in the frequency range between 1 kHz and 20 MHz, limited by the measurement method. The stream of pulses allows to extract any harmonics of the laser repetition rate, all phase locked to one another. The synchronization laser beam can be used to seed other lasers by generating higher harmonics of the 1550 nm. Due to the low repetition rate individual pulses can be used for electro-optical measurement to determine the bunch length or the beam arrival time (beam phase monitor) .

Fiber length stabilization: An RF phase lock loop comparing the back-reflected pulse with subsequent ones has demonstrated to be sufficient for a stabilization better than 20 fs. Using sum harmonic generation, the next step is to stabilize the optical path length to the fs-regime.

Laser to RF conversion: For synchronization in the order of 50 fs a photo-detector, bandpass-filter and RF amplifier is sufficient. To remove long term drifts and to achieve synchronization smaller than 10 fs, ultra-low noise VCO's and fiber loops controlled by optical phase modulators are planned.

In the final stage, the goal is to synchronize arbitrary points in (e.g. diag. laser, pump probe laser, VCO output, etc) better than 10 fs rms.

SUMMARY

Pump probe experiments with time stability of 30 fs rms become realistic, by further improvements of the low level RF regulations which allows amplitude and phase stability of $5 \cdot 10^{-5}$ and 0.01° within the pulse train. Mandatory for this timing stability is a laser based synchronization system that providing 10 fs point-to-point timing jitter to synchronize lasers and acceleration to one another.

REFERENCES

- [1] M. Hentschel *et al.*, "Attosecond metrology", Nature 414, 509-513 (2001)
- [2] E. Goulielmakis *et al.*, "Direct Measurement of Light Waves", Science, Vol. 305, 1267-1269 (2004)
- [3] B. Faatz, "First Results from the VUV FEL at DESY", PAC'05, May 2005, Tennessee
- [4] B. Steffen, "Spectral Decoding", FEL'05, August 2005, San Francisco
- [5] M. Dohlus, T. Limberg, "Bunch Compression Stability Dependence on RF Parameters", FEL'05, August 2005, San Francisco
- [6] F. Kaertner *et al.*, "Progress in Large Scale Femtosecond Timing Distribution and RF-Synchronization", PAC'05, May 2005, Tennessee
- [7] A. Winter, "Synchronization of Femtosecond Pulses", FEL'05, August 2005, San Francisco
- [8] A. Winter *et al.*, "Femtosecond Timing Distribution", FEL'05, August 2005, San Francisco